AIP Journal of Applied Physics

Scandium induced structural transformation and B′:B″ cationic ordering in Pb(Fe0.5Nb0.5)O3 multiferroic ceramics

B. Mallesham, R. Ranjith, and M. Manivelraja

Citation: Journal of Applied Physics **116**, 034104 (2014); doi: 10.1063/1.4890020
View online: http://dx.doi.org/10.1063/1.4890020
View Table of Contents: http://scitation.aip.org/content/aip/journal/jap/116/3?ver=pdfcov
Published by the AIP Publishing

Scandium induced structural transformation and B′:B″ cationic ordering in $Pb(Fe_{0.5}Nb_{0.5})O_3$ multiferroic ceramics

B. Mallesham,[1] R. Ranjith,[1,a)] and M. Manivelraja[2]
[1]*Department of Materials Science and Metallurgical Engineering, Indian Institute of Technology Hyderabad, Ordnance Factory Estate, Yeddumailaram 502205, India*
[2]*Defence Metallurgical Research Laboratory, Hyderabad 500058, India*

(Received 26 May 2014; accepted 1 July 2014; published online 17 July 2014)

The current study explores non-magnetic Sc^{3+} induced structural transformation, evolution of local B-site cation ordering and associated effect on ferroelectric phase transition temperature T_{max} (temperature corresponding to dielectric maxima) on increasing the atom percent of Sc substitution in $[Pb(Fe_{0.5}Nb_{0.5})O_3$ (PFN)] ceramics. In this regard, the phase pure $Pb[(Fe_{0.5-x}Sc_x)Nb_{0.5}]O_3$ ceramics with x varying from 0 to 0.5 were synthesized through solid state reaction route. The detailed structural analysis through Rietveld refinement confirms the room temperature transformation from a monoclinic Cm to rhombohedral R3m structure at $x = 0.3$ mol. % of Sc. Absorption spectra studies show that there is a considerable increment in the bandgap at higher scandium content. Most interestingly, the T_{max} exhibited an increment for lower scandium contents ($x = 0.1$ to 0.25) followed by a drop in T_{max} ($x = 0.3$ to 0.5). Such anomalous behavior in T_{max} is expected to arise due to the onset of B′, B″ local cation ordering beyond Sc content $x = 0.25$. The B-site cation ordering at and beyond $x = 0.3$ was also confirmed by the evolution of cation order induced Pb-O coupled vibrational mode in Raman scattering studies. In addition, the Mössbauer spectra of PFN ($x = 0$) and $Pb(Fe_{0.4}Sc_{0.1}Nb_{0.5})O_3$ ($x = 0.1$) are reported to verify the spin state and oxidation state of iron. The lattice distortion due to the radius ratio difference between a Sc^{3+} cation and Fe^{3+} cation in low spin state is responsible for the structural transformation, which in turn facilitates a B′:B″ cation ordering.
 [http://dx.doi.org/10.1063/1.4890020]

I. INTRODUCTION

Magnetoelectric multiferroic materials have attracted researchers due to their unique physical properties.[1,2] Materials that simultaneously possess more than one ferroic ordering are *termed multiferroics*.[1,2] Multiferroic relaxors exhibiting complex perovskite structure [General formula: $A(B'B'')O_3$, B′—low valence cation (Fe^{3+}), and B″—high valence cation (Nb^{5+}, Ta^{5+}, W^{6+})] like $Pb(Fe_{0.5}Nb_{0.5})O_3$, $Pb(Fe_{2/3}W_{1/3})O_3$, and $Pb(Fe_{0.5}Ta_{0.5})O_3$ were discovered in the early 1960s.[3–5] In such systems, the magnetic ordering arises due to the presence unpaired $3d^n$ electrons of Fe^{3+}, whereas the distortion introduced by $6s^2$ lone pair of Pb^{2+} on the B″ exhibiting d^0 configuration gives rise to ferroelectric ordering.[1,2,6,7]

Among these multiferroic relaxors, lead iron niobate $Pb(Fe_{0.5}Nb_{0.5})O_3$ [PFN] is much explored to understand its anomalous behavior in structural, electrical, and magnetic properties. PFN exhibits a ferroelectric phase transition (T_{max}) at ~380 K and antiferromagnetic phase transition (Neel temperature, T_N) around 143 K.[3–5,8–10] In recent studies, a magnetic spin anomaly has been observed at the onset of ferroelectric ordering, in spite of relatively low Neel temperature.[11] Such spin resonance spectroscopic studies in combination with magnetic studies, clearly establish a plausible interaction between the magnetic moments and the ferroelectric phonon modes present in PFN.[11] Hence, PFN is considered as a potential candidate to understand the basic science involved in the magneto-electric coupling in multiferroic relaxors. The room temperature crystal structure of PFN is proposed as Rhombohedral (space group: R3m)[12] as well as monoclinic (space group: Cm).[13–15] In addition, the dielectric studies of PFN reveal that it does not exhibit frequency dispersion in T_{max},[16–18] which is considered as one of the characteristic features of relaxor ferroelectrics (high dielectric constant, diffused phase transition, frequency dispersion in T_{max}, Ref. 19).

The earlier studies explain that lack of B-site cation ordering is responsible for the absence of frequency dispersion in T_{max} of PFN ceramics.[20,21] Randall *et al.*[21] reported that the scale of local ordering of B-site cation is crucial for these compounds to behave as a relaxor ferroelectric. Complex perovskites with local ordered regions between (<2 nm) and (≥100 nm) exhibit normal ferroelectric and/or antiferroelectric features, whereas perovskites with ordered regions between 2 nm to 50 nm exhibit relaxor features.[21] The local B-site cation ordering and frequency dispersion in T_{max} mainly depends on the ionic radius of B′ (ferroelectrically inactive) and B″ (ferroelectrically active) cations.[20] In case of oxides with B′ > B″, the ferroelectrically active B″ cation is weakly coupled to Pb-O-B″ bonding, as a consequence B″ induces distortion in the bonding along with Pb^{2+} lone pair, which initiates ordering of cation along ⟨111⟩ direction and hence most of the relaxors with B′ > B″ locally adopt R3m symmetry.[20] Hence, it is essential to look at the effect of cation ordering on physical properties of these disordered ceramics.

a)Author to whom correspondence should be addressed. Electronic mail: ranjith@iith.ac.in

There are few studies reporting effect of A-site and/or B-site substitution in PFN on the ferroelectric phase transition behavior, relaxor features, and magnetic properties.[18,22–26] Vershney *et al.* reported that Ba substituted PFN exhibits frequency dispersion in T_{max} due to compositional fluctuation at nanoscale.[18] The recent reports on (1-x)$Pb(Fe_{0.5}Nb_{0.5})O_3$-x$Ba(Fe_{0.5}Nb_{0.5})O_3$, (1-x)$Pb(Fe_{0.5}Nb_{0.5})O_3$-x$PbTiO_3$ solid solutions explored the effect of cation substitution on *Neel temperature* and *antiferromagnetic order*.[25,26] In the present study, polycrystalline Sc substituted $Pb[(Fe_{0.5-x}Sc_x)Nb_{0.5}]O_3$ compounds have been synthesized via conventional solid state route. The influence of scandium on structural and optical properties of these compounds is studied. Also, the scandium induced local B′: B″ cation ordering at higher scandium percent and its associated effect on ferroelectric phase transition temperature (T_{max}) of these ceramics have been explored.

II. EXPERIMENTAL DETAILS

In the present work, Pb $(Fe_{(0.5-x)}Sc_xNb_{0.5})O_3$ [x = 0, 0.1, 0.15, 0.2, 0.25, 0.3, 0.4, 0.5] powders were synthesized through solid state reaction route. The analytical grade precursors PbO, Fe_2O_3, Sc_2O_3, Nb_2O_5 (Make: sigma Aldrich, purity: ≥99.9%) were used to synthesize the phase pure $Pb(Fe_{(0.5-x)}Sc_xNb_{0.5})O_3$ powders. The two well-known problems in synthesizing lead based relaxor compounds are: formation of pyrochlore ($Pb_2Nb_2O_7$ or $Pb_3Nb_4O_{13}$) as a secondary phase and volatilization of lead during sintering. In order to minimize pyrochlore phase formation, the *wolframite precursor method*[17,27] was implemented and to reduce the lead loss while sintering 3 wt. % excess PbO was added during synthesis. Initially, wolframite precursors $FeNbO_4$, $ScNbO_4$ were prepared by grinding appropriate precursors in an agate mortar and calcination of homogeneously grinded precursors at 1200 °C for 6 h. Then, the single phase wolframite precursors and PbO were mixed homogeneously in stoichiometric proportions to obtain $Pb(Fe_{(0.5-x)}Sc_xNb_{0.5})O_3$ powders. Homogeneously mixed powders were calcined at 850 °C for 4 h followed by the phase confirmation of PFN and Sc substituted PFN. Phase pure powders were pressed to form a circular pellet of 6 mm diameter and thickness ≈1 mm, further sintered at 1050 °C for 4 h. The composition of all the sintered pellets utilized in the studies was confirmed by Energy dispersive X-ray spectroscopy analysis.

The structural and phase purity of the synthesized compounds were studied by powder X-ray diffractometer (PANalytical Xpert Pro) with CuK_α radiation. The Rietveld refinement of patterns was carried out using "Fullprof" software package to confirm the structure. The absorption spectral patterns of all the compositions were collected using UV-VIS-NIR-Spectrophotometer (Shimadzu, UV-3600). The dielectric properties (100 Hz-1 MHz) from room temperature to 200 °C were measured with an impedance analyzer (Agilent, 4294A). Mössbauer spectra were recorded using a constant acceleration spectrometer (FastCom Tech, Germany) with 25 mCi $^{57}Co(Rh)$ radio-active gamma ray source. The experimental data were analyzed using PCMOS-II least-squares fitting program. Raman spectra of all the sintered pellets were collected at room temperature using dispersive microscope spectrometer (SENTERRA, Bruker).

III. RESULTS AND DISCUSSION

Powder X-ray diffraction patterns of $Pb(Fe_{0.5}Nb_{0.5})O_3$, $Pb(Sc_{0.5}Nb_{0.5})O_3$ [PSN] (x = 0.5), and Sc substituted compounds confirm the absence of any secondary phase (like pyrochlore). Scandium substitution leads to an expansion of unit cell volume due to larger ionic radius of Sc^{3+} (74.5 pm) compared to Fe^{3+} (64.5 pm and 55 pm in high spin and low spin states, respectively).[28] The changes in unit cell dimensions are evidenced from the shifting of various peak positions towards lower Bragg angle with increasing scandium content [see Figures 1(a)–1(c)]. The structural refinement studies

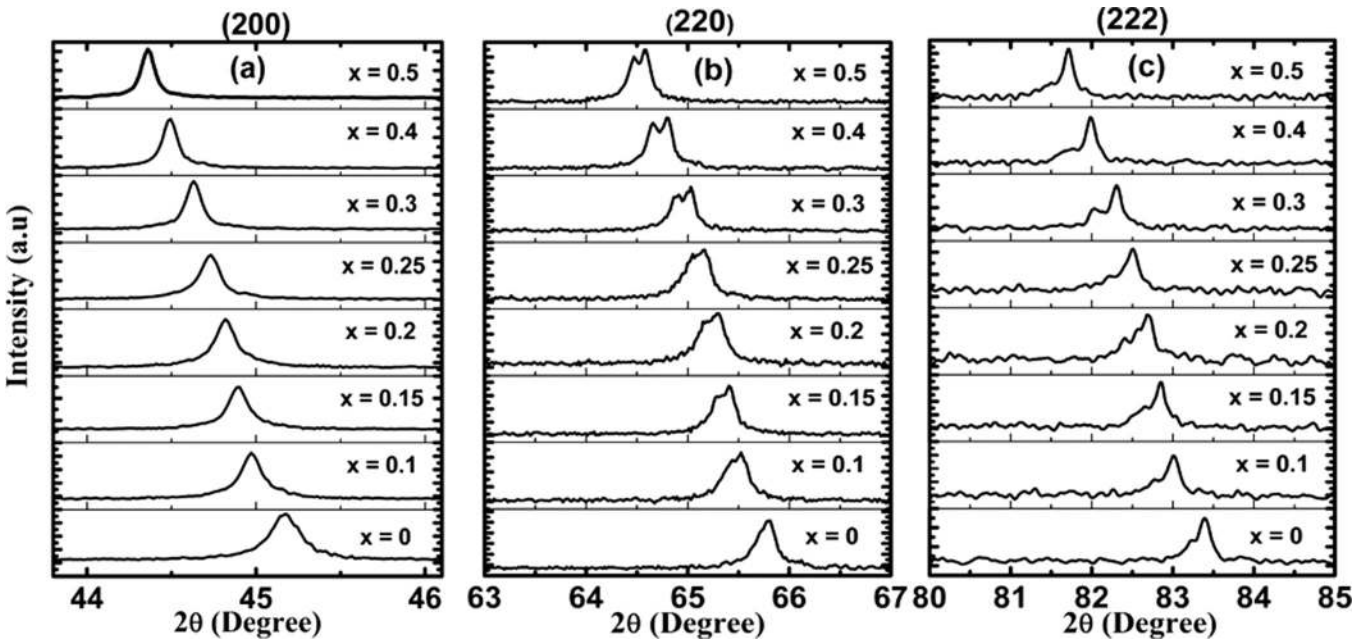

FIG. 1. Enlarged X-ray diffraction profiles of (a) (200), (b) (220), and (c) (222) reflections and Sc substituted compounds.

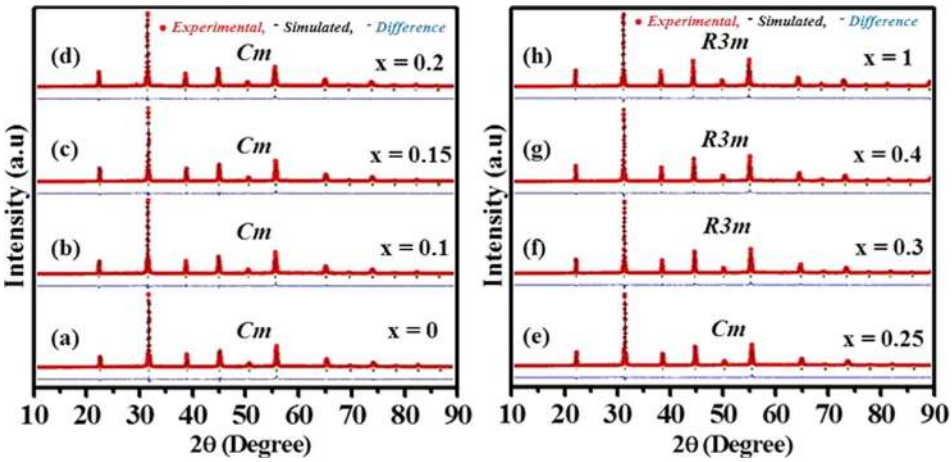

FIG. 2. Rietveld refined X-ray diffraction patterns.

performed on the powder diffraction pattern of PFN ceramics confirm that PFN stabilizes in a monoclinic symmetry (Cm) at room temperature, which is accordance with earlier studies.[13–15] However, the room temperature crystal structure of PSN ($x = 0.5$) stabilizes in rhombohedral (R3m) symmetry.[27,29] Figures 1(a)–1(c) show the enlarged profiles of (200), (220), and (222) reflections of all the compositions studied. In all these profiles, the associated $K\alpha_2$ peak has been stripped using standard Xpert-high score software. In all the compositions, (200) appears as a singlet, (220) and (222) exhibit doublet like characteristics with weak reflections at the lower 2θ. The pseudo cubic (200) reflection is broad and asymmetric in PFN ($x = 0$) and Sc substituted compositions up to $x \leq 0.25$. The anomalous broadening and asymmetry in (200) reflection are similar to earlier reports of $Pb(Fe_{0.5}Nb_{0.5})O_3$, $Pb(Zr_xTi_{1-x})O_3$, and $Pb(Mg_{1/3}Nb_{2/3})O_3-xPbTiO_3$,[15,30,31] which are attributed to monoclinic crystal structure with Cm space group. However, the anomalous peak broadening and asymmetry of (200) reflection disappear for compositions $x \geq 0.3$. The sharp (200) reflection without any asymmetry in peak is attributed to rhombohedral crystal structure with R3m space group.[15,31] However, in order to confirm the crystal structure the Rietveld refinement of the experimental powder diffraction patterns of all the compositions is carried using *Fullprof suite package* [*2013 version*].

The Rietveld refinement of PFN ($x = 0$) and Sc substituted compounds up to $x \leq 0.25$ was performed by assigning Cm (monoclinic symmetry) crystallographic space group model.[14] Figures 2(a)–2(e) show the refined patterns of compositions with monoclinic symmetry. In Table I, the refined unit-cell parameters, Goodness of fit ($\chi 2$) of all the compositions with monoclinic symmetry have been provided. The obtained goodness of fit confirms that for Sc substitution up to $x = 0.25$ mol. % the system retains the parent crystal symmetry. Whereas the refinement of solid solutions in the range of $0.3 \leq x \leq 0.5$ reveals the dominance of Sc induced distortion and hence adopts the structure of pure PSN compound with R3m symmetry. Figure 2(f)–2(h) shows the refined patterns of compositions with rhombohedral symmetry. Refined structural parameters of compositions with rhombohedral symmetry are provided in Table II. Hence, the detailed structural refinement studies of all the compositions reveal that Sc induced distortion transforms the monoclinic crystal structure of PFN to rhombohedral at $x = 0.3$ mol. % of scandium. To refine the rhombohedral phase, we have used hexagonal axes lattice parameters reported by Perrin *et al.*[27] The refined hexagonal cell parameters of R3m crystallographic model are converted into

TABLE I. Refined parameters of $Pb(Fe_{0.5-x}Sc_xNb_{0.5})O_3$ compositions with monoclinic (Cm) symmetry.

Composition	Unit cell parameter				R_B	χ^2
	a (Å)	b (Å)	c (Å)	β (deg)		
$x = 0$	5.675	5.671	4.018	89.89	8.028	2.47
$x = 0.1$	5.699	5.692	4.032	89.87	6.778	2.02
$x = 0.15$	5.709	5.702	4.039	89.85	6.488	2.03
$x = 2$	5.719	5.711	4.046	89.85	6.460	2.13
$x = 0.25$	5.730	5.722	4.054	89.84	7.058	2.18

Refined positional coordinates and thermal parameters of $x = 0$ (PFN)

Ions	Positional coordinates			Thermal parameters B_{iso} (Å^2)
	X	Y	Z	
Pb^{2+}	0	0	0	2.92
Fe^{3+}/Nb^{5+}	0.477	0	0.482	0.849
O1	0.46	0	−0.03	0.6
O2	0.212	0.242	0.418	0.6

TABLE II. Refined parameters of $Pb(Fe_{0.5-x}Sc_xNb_{0.5})O_3$ compositions with Rhombohedral (R3m) symmetry.

Composition	Unit cell parameter				R_B	χ^2
	a_h (Å)	c_h (Å)	a_R (Å)	α_R (deg)		
$x = 0.3$	5.734	7.042	4.058	89.90	10.99	2.26
$x = 0.4$	5.752	7.065	4.071	89.90	9.634	2.22
$x = 5$	5.768	7.083	4.082	89.90	10.46	2.17

Refined positional coordinates and thermal parameters of $x = 0.5$ (PSN)

Ions	Positional coordinates			Thermal parameters B_{iso} (Å^2)
	X	Y	Z	
Pb^{2+}	0	0	0.492	2.73
Sc^{3+}/Nb^{5+}	0	0	0.019	1.03
O	0.384	0.176	0.130	1.9

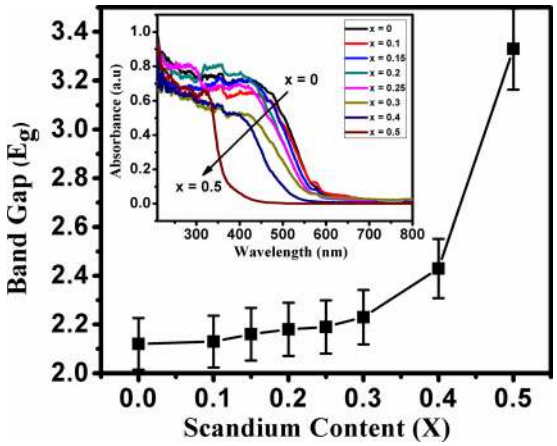

FIG. 3. Variation of band gap with scandium content [inset shows the absorption spectra of $Pb(Fe_{0.5-x}Sc_xNb_{0.5})O_3$ (x = 0, 0.1,0.15, 0.2, 0.25, 0.3, 0.4, 0.5).

rhombohedral cell parameters [provided in Table II] in accordance with following equations:[32]

$$a_R = \frac{1}{3}\sqrt{3a_H^2 + c_H^2}, \tag{1}$$

$$\alpha_R = 2\sin^{-1}\left(\frac{3}{2\sqrt{3 + (c_H/a_H)^2}}\right). \tag{2}$$

Figure 3 shows the variation of optical band gap with increase of scandium content. The band gap of the pure and solid solutions was obtained by Tauc and Wood relation[33] at the absorption edge (figure inset shows the complete absorption spectra of all compounds studied). The estimated band gap increases with increasing the scandium content from 2.1 ± 0.05 eV (x = 0) to 3.3 ± 0.05 (x = 0.5). The influence of scandium substitution is not prominently affecting the absorption features for lower atom percent of scandium. However, the increment in band gap at higher concentrations is predominant which could be attributed to the $3d^0$ configuration of the Sc^{3+} cation. The effect of band gap increment on high atom percent of Sc substitution in PFN is reflected on the reduction of dielectric losses, which will be discussed later.

Figure 4(a) shows the variation of normalized dielectric constant with temperature for PFN, PSN, and $Pb(Fe_{0.25}Sc_{0.25}Nb_{0.5})O_3$. Ferroelectric phase transition temperature (T_{max}) for both PFN and PSN were found to be 378 K and 368 K, respectively, which is accordance with the literature.[10,29] The inset of Figure 4(a) shows the variation of real and imaginary parts of dielectric constant with temperature measured at high frequency (1 MHz). The high frequency data have been reported to exclude the extrinsic contributions on dielectric polarization.[34,35] The dielectric studies reveal the presence of a broad and diffused phase transition, which is a common feature of such compounds. The dielectric loss (ε'') of the compounds decreased with increasing scandium content (see inset Figure 4(a)). The high dielectric loss in PFN and PFN with lower scandium content might be due to lower band gap. The phase transition temperature (T_{max}) exhibited an anomalous behavior with varying composition. T_{max} increases initially with increasing scandium content up to 403 K (for x = 0.25), later decreases as the scandium content increases as shown in Figure 4(b).

Figure 4(b) shows a linear variation of T_{max}, which was calculated from the empirical relation given in Eq. (3) for solid solutions of similar perovskite compounds.[36]

$$T\text{max} = x(368\text{K}) + (1-x)(378\text{K}). \tag{3}$$

In this study, the constituent compounds are PFN, PSN and there T_{max} are 378 K, 368 K, respectively. Substituting these experimental values of T_{max} in Eq. (3) (Ref. 36), the variation of T_{max} with respect to the Sc content (at. %) was calculated and plotted. The variation of T_{max} is expected to be a linear curve as seen in Figure 4(b) (calculated). However, the experimental evidences prove that no such linear variation of T_{max} could be observed with respect to the scandium content in PFN ceramics. Interestingly, the T_{max} exhibited an increment as a function of Sc content up to 1:1 ratio of Fe and Sc. Later for Sc content above x = 0.25, the T_{max} showed a declining feature. Such observation of raise and fall of T_{max} is not commonly observed in similar ferroelectric solid solutions.[36–38] There are few reports on solid solutions, which do not exhibit linear relationship between T_{max} with the respective substitution content x (at. %);[23,39] however, the origin of such behavior was left ambiguous. The ferroelectric phase transition temperature (T_{max}) of PSN is known to be associated with B′:B″ cation ordering processed under ambient conditions. The process induced B′:B″ cation ordering in PSN like compounds reveals that the disordered state could induce an increment in T_{max} compared to ordered state.[29] In addition, the local cation ordering is known to be plausible when ionic radius of B′ > B″, whereas when the ionic radius of B′ < B″ no local cation ordering could be detected (like PFN).[20,21]

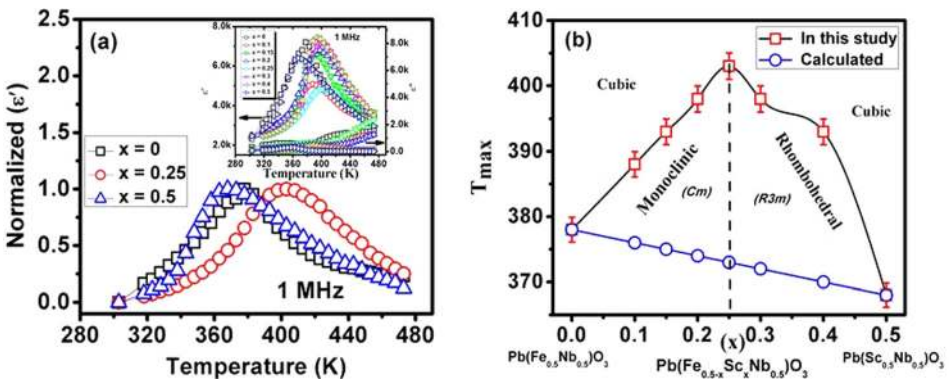

FIG. 4. (a) Variation of normalized dielectric constant (ε') with temperature for x = 0, 0.25, and 0.5, [inset: Variation of real (ε'), imaginary (ε'') parts of dielectric constant with temperature of $Pb(Fe_{0.5-x}Sc_xNb_{0.5})O_3$]. (b) Variation of ferroelectric phase transition temperature (T_{max}) with varying scandium content (x), both experimental (open square) and empirically calculated[36] (open circles).

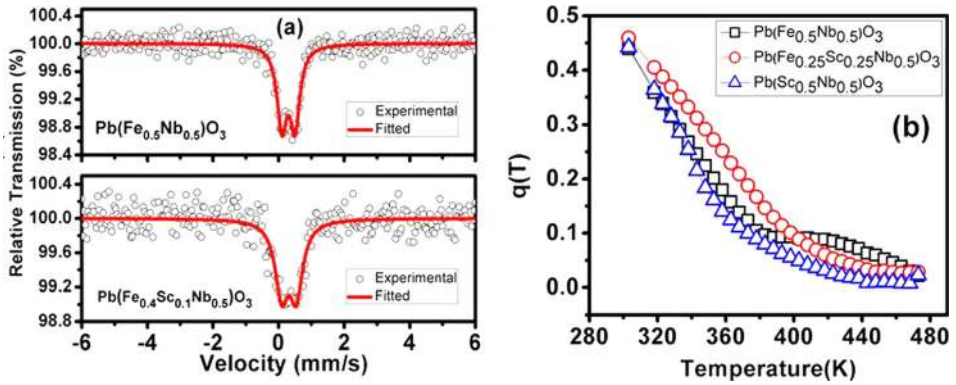

FIG. 5. (a) Mössbauer spectra of $Pb(Fe_{0.5}Nb_{0.5})O_3$ and $Pb(Fe_{0.4}Sc_{0.1}Nb_{0.5})O_3$ displaying doublet. (b) Variation of local order parameter q with temperature calculated using Eq. (5) at 1 MHz.

In the case of PFN, ionic radius of Fe^{3+} is known to vary with the spin state of the cation,[28] so the spin state of the Fe^{3+} was verified using Mössbauer spectroscopy. The oxidation states (Fe^{2+}, Fe^{3+}) and spin states (low, high) can be studied using Mössbauer hyperfine parameters such as isomer shift (I.S.) and quadrupole splitting (Q.S.). Figure 5(a) shows the Mössbauer spectra recorded for the pure PFN and $Pb(Fe_{0.4}Sc_{0.1}Nb_{0.5})O_3$ (PFSN) ($x = 0.1$) compounds. The spectra were fitted with only one doublet with low isomer shift and quadrupole splitting values. The obtained I.S. and Q.S. values of PFN, PFSN show there is no change in the spin state with Sc substitution [hyperfine parameters are shown in Table III]. Also hyperfine parameters reveal the absence of any mixed oxidation state of iron cation and also confirm that the Fe^{3+} is present in low spin state (I.S. < 0.35 mm/s). Hence, the B′ cation radius ($r_{Fe3+} = 55$ pm)[28] is lesser than that of B″ cation radius ($r_{Nb5+} = 64$ pm)[28] in the case of PFN. Hence, in PFN there is no detectable B-site cation ordering due to smaller cationic radius of B′ compared to B″.[20,21] In addition, the stabilization of PFN with monoclinic symmetry does not facilitate a B cation distortion favored along the ⟨111⟩ direction. Due to the lack of B-site cation ordering, local field associated with polarizability of Pb^{2+} is large and sufficiently distributed over the random environment. But, in the case of pure PSN, the ionic radius of the B′ cation, i.e., the Sc^{3+} (74.5 pm)[28] is larger than the B″ cation, i.e., the Nb^{5+} (64 pm)[28] and possesses a long range B′:B″ cation ordering with a T_{max} of 368 K. The influence of cation ordering on the T_{max} reveals that PSN ceramic with long range B′-B″ cation ordering exhibits a lower T_{max} (360 K) in comparison to the phase with disordered (~380–390 K) B-site cation.[29] In this study, the T_{max} of PSN ceramics was found to be around 368 K, which is close to the B-site ordered phase of PSN. In addition, the rhombohedral symmetry of the PSN ceramics facilitates the B′:B″ cation ordering along the ⟨111⟩ direction.[20]

In this study, the compounds with monoclinic symmetry Cm (PFN) exhibit lack of B-site cation ordering. However, compounds with higher Sc content ($x \geq 0.3$) attain the R3m symmetry and exhibit a structurally driven local 1:1 ordering of B′ (Sc^{3+}/Fe^{3+}) and B″ (Nb^{5+}) cations.[20] So the initial rise of T_{max} up to Sc content ($x \leq 0.25$) could be attributed to the large and sufficiently distributed local field due to lack of B-site cation ordering. Whereas the fall in T_{max} beyond the Sc content ($x \geq 0.3$) might be due to the onset of local B-cation ordering, in which the local field has a narrow or negligible distribution.[20] The dependence of ferroelectric phase transition temperature (T_{max}) on local structure was investigated by Grinberg *et al.* and Juhas *et al.* in $Pb(Zn_{1/3}Nb_{2/3})O_3$–$PbTiO_3$, $Pb(Mg_{1/3}Nb_{2/3})O_3$–$PbTiO_3$, $Pb(Sc_{2/3}W_{1/3})O_3$–$PbTiO_3$, $Pb(Sc_{2/3}W_{1/3})O_3$–$PbZrO_3$ solid solutions through density functional theory.[40,41] A strong relation between the low temperature cation displacements and ferroelectric phase transition temperature (T_{max}) of a relaxor with heterogeneous B cation was proposed, as shown below.[40,41]

$$T_{max} = ad_{Pb}^2 + bd_{B'/B''}^2 f_{B'/B''}, \quad (4)$$

where d_{Pb} is the average magnitude of the Pb distortion, $d_{B'/B''}$ is the average magnitude of distortion of the ferroelectrically active B cation, $f_{B'/B''}$ is the fraction of the ferroelectrically active B cations in solution and a, b are the constants. In the present study, Sc^{3+} substitution at Fe^{3+} site weakens the Pb-O-Nb coupling due to its higher ionic radius compared to Nb^{5+}. This facilitates the cooperative displacement of Nb^{5+} cations along with Pb^{2+} in a disordered sate. This leads to enhanced polarization and as a consequence high dielectric response drives up the T_{max} until B-site cation ordering begins. In ordered state, the average length of the Pb-O-Nb bonds reduces, as a result relative displacement of Pb^{2+} and Nb^{5+} decreases and thus leads to lowering of T_{max}. So in the present study T_{max} increases up to $x = 0.25$ mol. % of Sc content and decreases from $x = 0.3$ due to the beginning of local cation ordering. Raman scattering studies show evidence for local cation ordering beyond $x \geq 0.3$, which will be discussed later.

TABLE III. Hyperfine parameters obtained from Mössbauer spectra of $Pb(Fe_{0.5}Nb_{0.5})O_3$ [PFN] $Pb(Fe_{0.4}Sc_{0.1}Nb_{0.5})O_3$ [PFSN] sintered at 1050 °C for 4 h. [I.S: Isomer shift, Q.S: Quadrupole splitting].

S. No	Compound	I.S (mm/s)	Q.S (mm/s)	WV (mm/s)	INT. (%)	Chemical nature
1.	$Pb(Fe_{0.5}Nb_{0.5})O_3$	0.302 ± 0.007	0.39 ± 0.01	0.36 ± 0.02	100	Fe^{3+}
2.	$Pb(Fe_{0.4}Sc_{0.1}Nb_{0.5})O_3$	0.317 ± 0.010	0.44 ± 0.03	0.48 ± 0.04	100	Fe^{3+}

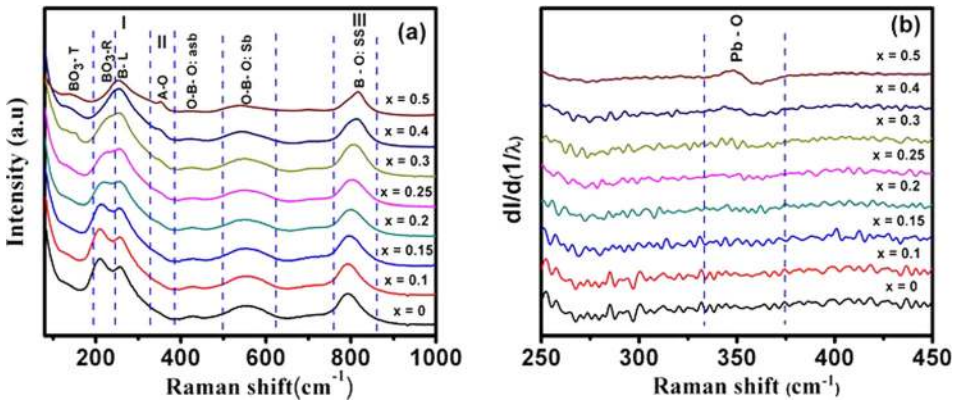

FIG. 6. (a) Raman spectra of $Pb(Fe_{0.5-x}Sc_xNb_{0.5})O_3$ [ss: symmetric stretching, sb: symmetric bending, asb: asymmetric bending, R: Rotation, T: Translation, L: localized]. (b) Derived pattern of Pb-O vibrational mode.

The strength of ferroelectric dipole–dipole interactions could also be evidenced from the local order parameter q [correlation parameter] of a disordered system. The local order parameter of a spin glass (a disordered magnetic system with competing interactions) introduced by Sherrington and Kirkpatrick[42] was also utilized to explain the dielectric glassy behavior of relaxor ferroelectrics.[43] According to this model, the temperature dependence of susceptibility [χ] below T_f relates to local order parameter as given in the following equation:

$$\chi = \frac{C\left[1 - q(T)\right]}{T - \theta\left[1 - q(T)\right]}, \tag{5}$$

where C, θ were determined from the high temperature Curie-Weiss analysis. In analogy to spin glass, the local order parameter indicates the onset of local polar clusters and the presence of correlation among these clusters in relaxors like $Pb(Mg_{1/3}Nb_{2/3})O_3$. The presence of correlation among polar clusters leads to deviation from normal Curie–Weiss behavior above T_{max} and until the onset of local polar clusters (T_{Burns}).[43] In the present work, we have estimated the local order parameter of $Pb(Fe_{0.5}Nb_{0.5})O_3$ [$T_{max} = 378$ K], $Pb(Sc_{0.5}Nb_{0.5})O_3$ [$T_{max} = 363$ K], and $Pb(Fe_{0.25}Sc_{0.25}Nb_{0.5})O_3$ [$T_{max} = 403$ K] compositions using Eq. (5). Figure 5(b) shows the temperature dependence of local order parameter. In the figure, it is clearly seen that q decreases linearly in all the compositions with temperature until their respective T_{max}. Then, it decreases non-linearly and flattens to zero around 440 K. The abnormal variation of q after T_{max} in PFN compound might be due to dominant leakage behavior. In addition, the magnitude of local order parameter of $Pb(Fe_{0.25}Sc_{0.25}Nb_{0.5})O_3$ is higher than that of the other compounds. This indicates the presence of strong correlation between neighboring moments in $Pb(Fe_{0.25}Sc_{0.25}Nb_{0.5})O_3$ as commonly observed in highly cationic disordered relaxor ferroelectrics. Hence, the increment in T_{max} of $Pb(Fe_{0.25}Sc_{0.25}Nb_{0.5})O_3$ compared to all other compositions could be attributed to the distribution of these strong correlation strengths over random fields.

Figure 6(a) shows the room temperature Raman spectra of $Pb(Fe_{0.5-x}Sc_xNb_{0.5})O_3$. The spectra have been divided into three frequency regions (region I: 200–300 cm^{-1}, region II: 300–400 cm^{-1}, and region III: 750–850 cm^{-1}) based on observed changes in vibrational modes for convenience in discussion. The vibrational mode in *region III* corresponds to vibration of oxygen atom along the B′-O-B″ linkage with all the cations at rest, it is also represented as symmetric stretching of B′-O, B″-O bonds.[44,45] In the present spectra, symmetric stretching mode (around 800 cm^{-1}) shifts towards higher frequency with increasing Sc content. The shift in frequency due to scandium might be attributed to lower atomic mass of scandium compared to iron or due to the changes in restoring forces experienced by the oxygen. The presence of B-site local ordering can also be evidenced from this mode based on intensity and sharpness of peak.[44] The vibrational mode in *region II* around 350 cm^{-1} is attributed to O vibrations along Pb-O bonds due to the electron phonon coupling of the Pb^{2+} lone pair electrons.[38,44,45] Figure 6(b) shows the derived spectra of region II. The derived spectra of this vibrational mode clearly indicate that this mode was absent in pure PFN (x = 0) and lower scandium content compounds, evolution of this mode begins at x = 0.3 of scandium content. The evolution of Pb-O mode mainly associated with the long range coupled Pb-O ferroic species.[46] Hence, strength of coupling between Pb-O ferroic species decides the degree of orientational ordering of lone pairs, consequently size of the local B-site ordered regions.[38,44–46] From this observation, we can ensure that scandium drives a local ordering at B-site, which was absent in PFN (x = 0). Also, there is a considerable change in the vibrational modes of ***region I*** with increasing scandium content. In this regime, there are two vibrational modes centered around 200 cm^{-1} and 250 cm^{-1} belonging to rotation of octahedra and localization of B-cation, respectively.[44,45] In PFN (x = 0), both the vibrational modes are clearly visible, but as the scandium content increases the octahedra rotational mode superimposes with the B-localized mode then appears as a single vibrational mode at higher scandium percentages. Since the vibrational mode corresponding to rotation of octahedra is more sensitive to the crystal symmetry, the two modes appearing for the monoclinic symmetry merge to a single mode when the system transforms to rhombohedral.

IV. CONCLUSION

In conclusion, $Pb[(Fe_{0.5-x}Sc_x)Nb_{0.5}]O_3$ solid solutions were synthesized using wolframite precursor method and the structural studies confirmed that there is a transformation from monoclinic (Cm) to rhombohedral (R3m) at

$x = 0.3$ mol. % of scandium. In addition, the larger cationic radius of Sc^{3+}(74.5 pm) in comparison with Fe^{3+}(55 pm) in low spin state is expected to drive a structurally facilitated cationic ordering due to the rhombohedral symmetry at higher scandium content ($x \geq 0.3$). The unconventional behavior of T_{max} in these solid solutions is mainly associated with B-site cation local ordering and coupling strength of ferroelectrically active Nb^{5+} with Pb-O-Nb bonding. The initial rise in T_{max} with increasing Sc content until $x = 0.25$ mol. % is due to lack of cation ordering and weak Pb-O-Nb bonding enhances the relative displacement of Pb^{2+} and Nb^{5+}, as a consequence T_{max} increases until local cation ordering begins. The fall in T_{max} from $x \geq 0.3$ mol. % of scandium is due to the onset of cation ordering. The cation ordering leads to shorter relative displacement Pb^{2+} and Nb^{5+}, which results in decrement of dielectric response. So T_{max} decreases from $x = 0.3$ mol. % of Scandium as the degree of cation ordering increases. The effect of cation ordering is evidenced through the evolution of Pb-O vibrational mode in the Raman spectra, which confirms the onset of B-site cation ordering at $x = 0.3$ at. % of Sc content.

ACKNOWLEDGMENTS

One of the authors R. Ranjith would like to acknowledge DST-India Fast Track scheme for the funding of the project. The authors also acknowledge Dr. Manish K. Niranjan for his feedback and comments on improving the manuscript.

[1]W. Eerenstein, N. D. Mathur, and J. F. Scott, Nature (London) **442**, 759 (2006).
[2]K. F. Wang, J. M. Liu, and Z. F. Ren, Adv. Phys. **58**, 321 (2009).
[3]G. A. Smolenskii, A. Agranovskaya, S. N. Popov, and V. A. Isupov, Sov. Phys. Tech. Phys. **28**, 2152 (1958).
[4]V. A. Vokov, I. E. Mylnikova, and G. A. Smolenskii, Sov. Phys. JETP **15**, 447 (1962).
[5]A. Kumar, R. S. Katiyar, C. Rinaldi, S. G. Lushinikov, and T. A. Shaplygina, Appl. Phys. Lett. **93**, 232902 (2008).
[6]D. Khomskii, Physics **2**, 20 (2009).
[7]N. A. Hill, J. Phys. Chem. B **104**, 6694 (2000).
[8]Y. Yang, J. M. Liu, H. B. Huang, W. Q. Zou, P. Bao, and Z. B. Liu, Phys. Rev. B **70**, 132101 (2004).
[9]M. H. Lente, J. D. S. Guerra, G. K. S. De Souza, B. M. Fraygola, C. F. V. Raigoza, D. Garcia, and J. A. Eiras, Phys. Rev. B **78**, 054109 (2008).
[10]O. Raymond, R. Font, N. Suarez-Almodovar, J. Portelles, and J. M. Siqueiros, J. Appl. Phys. **97**, 084107 (2005).
[11]R. Blinc, P. Cevc, A. Zorko, J. Holc, M. Kosec, Z. Trontelj, J. Pirnat, N. Dalal, V. Ramachandran, and J. Krzystek, J. Appl. Phys. **101**, 033901 (2007).
[12]S. A. Ivanov, R. Tellgren, H. Rundlof, N. W. Thomas, and S. Ananta, J. Phys: Condens. Matter **12**, 2393 (2000).
[13]V. Bonny, M. Bonin, P. Sciau, K. J. Schenk, and G. Chapuis, Solid State Commun. **102**, 347 (1997).
[14]N. Lampis, P. Sciau, and A. G. Lehmann, J. Phys: Condens. Matter **11**, 3489 (1999).
[15]S. P. Singh, D. Pandey, S. Yoon, S. Baik, and N. Shin, Appl. Phys. Lett. **90**, 242915 (2007).
[16]L. Yan, J. Li, and D. Viehland, J. Appl. Phys. **101**, 104107 (2007).
[17]S. P. Singh, S. M. Yusuf, S. Yoon, S. Baik, N. Shin, and D. Pandey, Acta Mater. **58**, 5381 (2010).
[18]D. Vershney, R. N. Choudhary, and R. S. Katiyar, Appl. Phys. Lett. **89**, 172901 (2006).
[19]K. Uchino, *Ferroelectric Devices* (Marcel Dekker, Inc., New York, 2000), p. 108.
[20]I. W. Chen, P. Li, and Y. Wang, J. Phys. Chem. Solids **57**, 1525 (1996).
[21]C. A. Randall, A. S. Bhalla, T. R. Shrout, and L. E. Cross, J. Mater. Res. **5**, 829 (1990).
[22]V. V. Bhat, A. M. Umarji, V. B. Shenoy, and U. V. Waghmare, Phys. Rev. B **72**, 014104 (2005).
[23]M. H. Lee and W. K. Choo, J. Appl. Phys. **52**, 5767 (1981).
[24]A. Levstik, C. Filipic, V. Bobnar, J. Holc, S. Drnovsek, Z. Trontelj, and Z. Jaglicic, J. Appl. Phys. **104**, 054113 (2008).
[25]I. P. Raevski, S. P. Kurbrin, S. I. Raevskaya, V. V. Titov, D. A. Sarychev, M. A. Malitskaya, I. N. Zakharchenko, and S. A. Prosandeev, Phys. Rev. B **80**, 024108 (2009).
[26]V. V. Lagutta, M. D. Glinchuk, M. Marysko, R. O. Kuzian, A. Prosandeev, S. I. Raevskaya, V. G. Smotrakov, V. V. Eremkin, and I. P. Raevski, Phys. Rev. B **87**, 064403 (2013).
[27]C. Perrin, N. Menguy, E. Suard, Ch. Muller, C. Caranoni, and A. Stepanov, J. Phys: Condens. Matter **12**, 7523 (2000).
[28]R. D. Shannon, Acta Crystallogr., Sect. A **32**, 751 (1976).
[29]C. Malibert, B. Dkhil, J. M. Kiat, D. Durand, J. F. Berar, and A. S. Bire, J. Phys.: Condens. Matter **9**, 7485 (1997).
[30] Ragini, R. Ranjan, S. K. Mishra, and D. Pandey, J. Appl. Phys. **92**, 3266 (2002).
[31]A. K. Singh and D. Pandey, Phys. Rev. B **67**, 064102 (2003).
[32]B. D. Cullity, *Elements of X-Ray Diffraction* (Addition Wesley Publishing Company, Inc., 1956), Appendix 2, p. 463.
[33]D. L. Wood and J. Tauc, Phys. Rev. B **5**, 3144 (1972).
[34]G. Catalan, D. O. Neill, R. M. Bowman, and J. M. Gregg, Appl. Phys. Lett. **77**, 3078 (2000).
[35]S. B. Majumder, S. Bhattacharyya, R. S. Katiyar, A. Manivannan, P. Dutta, and M. S. Sheehra, J. Appl. Phys. **99**, 024108 (2006).
[36]N. Vittayakorn, G. Rujijanagul, X. Tan, M. A. Marquardt, and D. P. Cann, J. Appl. Phys. **96**, 5103 (2004).
[37]Z. G. Ye, B. Noheda, M. Dong, D. Cox, and G. Shirane, Phys. Rev. B **64**, 184114 (2001).
[38]M. Correa, R. N. P. Choudhary, and R. S. Katiyar, J. Appl. Phys. **101**, 054116 (2007).
[39]S. Nomura, S. J. Jang, L. E. Cross, and R. E. Newnham, J. Am. Ceram. Soc. **62**, 485 (1979).
[40]I. Grinberg and A. M. Rappe, Phys. Rev. B **70**, 220101R (2004).
[41]P. Juhas, I. Grinberg, A. M. Rappe, W. Dmowski, T. Egami, and P. K. Davies, Phys. Rev. B **69**, 214101 (2004).
[42]D. Sherrington and S. Kirkpatrick, Phys. Rev. Lett. **35**, 1792 (1975).
[43]D. Viehland, S. J. Jang, L. E. Cross, and M. Wuttig, Phys. Rev. B **46**, 8003 (1992).
[44]D. Rout, V. Subramanian, K. Hariharan, and V. Sivasubramanian, Solid State Commun. **141**, 192 (2007).
[45]B. Guttler, B. Mihailova, R. Stosch, U. Bismayer, and M. Gospodinov, J. Mol. Struct. **661**, 469 (2003).
[46]N. Waeselmann, B. Mihailova, M. Gospodinov, and U. Bismayar, J. Phys: Condens. Matter **25**, 155902 (2013).